Journal of Nuclear Materials 386–388 (2009) 1087–1090

Contents lists available at ScienceDirect

Journal of Nuclear Materials

journal homepage: www.elsevier.com/locate/jnucmat

# Modeling of Li diffusivity in $Li_2O$ by molecular dynamics simulation

Takuji Oda *, Satoru Tanaka

*Department of Nuclear Engineering and Management, The University of Tokyo, 7-3-1 Hongo, Bunkyo-ku, Tokyo 113-8565, Japan*

A B S T R A C T

In order to understand the Li diffusion behavior in lithium-containing oxides under fusion-reactor conditions, classical molecular dynamics simulation was conducted for $Li_2O$. Fast Li diffusion, namely superionics, was clearly observed at temperatures higher than about half the melting point. In systems containing Li defects such as Li vacancies and Schottky-type defects, Li diffusion was promoted by these defects. It was indicated that both dynamic Frenkel defects, which are thought to induce superionics, and Li radiation defects created as a consequence of Li burn-up play important roles in Li diffusion under fusion-reactor conditions. The role of radiation defects is more significant in a system of higher Li burn-up and lower temperature.



## 1. Introduction

One of the essential steps for developing fusion reactors is the establishment of a safe and efficient fuel cycle using the breeding blanket. When using solid tritium breeders such as $Li_2TiO_3$ and $Li_4SiO_4$, the performance is influenced by radiation defects formed by high energy/flux neutrons. Hence, the radiation damage process in lithium-containing oxides has been regarded as an important research subject.

In the radiation damage process, the diffusion of the constituent atoms plays a key role, because it is relevant to the annihilation and aggregation of radiation defects. In the case of lithium-containing ionic crystals, Li often shows complicated fast diffusion. This phenomenon is called 'superionics,' and is thought to be induced by dynamic Frenkel defects [1]. Indeed, Li superionics has been observed in $Li_2O$ [1–3] and $Li_4SiO_4$ [4]. Moreover, the diffusion of the constituent atoms is basically promoted by radiation defects created under fusion-reactor conditions. Hence, not only dynamic Frenkel defects but also radiation defects should be considered when modeling Li diffusion in lithium-containing oxides under fusion-reactor conditions.

In the present work, therefore, we conducted classical molecular dynamics (MD) simulation for $Li_2O$, in order to understand and model the Li diffusion behavior in lithium-containing oxides under fusion-reactor conditions. For this purpose, the diffusion coefficients of Li were first evaluated in several systems having different defect concentrations: $Li_{1000}O_{500}$ (perfect $Li_2O$ crystal), $Li_{499}O_{500}$ (defective $Li_2O$ crystal containing 0.1% $Li^+$ vacancies), $Li_{1001}O_{500}$ (defective $Li_2O$ crystal containing 0.1% $Li^+$ interstitial ions) and $Li_{998}O_{499}$ (defective $Li_2O$ crystal containing 0.2% $Li^+$ vacancies and 0.2% $O^{2-}$ vacancies as Schottky-type defects). Then, the Li diffusivity was divided into three components which were separately analyzed: (i) Li diffusion assisted by dynamic Frenkel defects, (ii) that by radiation defects, and (iii) that by thermally induced defects excluding dynamic Frenkel defects. Each component was individually described by means of Arrhenius' type formula. Finally, the contribution of each component to the overall Li diffusivity was estimated under various reactor conditions, where Li defects were introduced as a consequence of Li burn-up.

## 2. Computational methods

The potential model-dependence of the simulation results is an essential shortcoming of classical MD simulation. In the present study, two Buckingham-type potential models were used and the results were compared, in order to eliminate improper results that artificially appear in a certain potential model. The Buckingham-type pairwise potential model between two ions is expressed as follows:

$$U(r) = \frac{q_1 q_2}{r} + A\exp\left(-\frac{r}{\rho}\right) - \frac{C}{r^6}. \quad (1)$$

Here, $r$ is the distance between two ions, $q_1$ and $q_2$ are their effective charges, and $A$, $\rho$ and $C$ are potential model parameters. One set of model parameters ($A$, $\rho$ and $C$ for the Li–Li, Li–O and O–O interactions) has been chosen so as to fit the potential energy curves evaluated by the *ab initio* calculation (plane-wave pseudopotential DFT with LDA functional) [5], and the other has been empirically determined so as to yield crystalline properties (*e.g.*, the lattice constant or elastic constants) close to the experimental values [6]. These two models are hereafter referred to 'FIT-LDA' and 'FIT-EMP,' respectively. As a feature, FIT-LDA describes inter-ionic interaction more strongly than FIT-EMP [6].

* Corresponding author. Tel./fax: +81 3 5841 6970.
*E-mail address:* oda@flanker.q.t.u-tokyo.ac.jp (T. Oda).

0022-3115/$ - see front matter © 2009 Elsevier B.V. All rights reserved.
doi:10.1016/j.jnucmat.2008.12.294

For the MD simulation, the *DL-POLY* code [7] was used. All calculations were conducted in a $5 \times 5 \times 5$ supercell ($Li_{1000}O_{500}$, $Li_{999}O_{500}$, $Li_{1001}O_{500}$ and $Li_{998}O_{499}$) under the three-dimensional periodic boundary condition. The Verlet leapfrog scheme [8] was applied to update the velocity and position of each atom under the Berendsen NPT ensemble [9]. The Coulombic term was evaluated by the Ewald summation technique [8], while the short-range interaction described by the Buckingham model was directly calculated using a cutoff distance of 10 Å.

The Li diffusion coefficients were acquired from the mean square displacement of Li. The time step was set to 1 fs, and the total simulation time was determined so that the error of the evaluated diffusion coefficient was suppressed around several percent. This error level was typically achieved by simulation lasting a few nanoseconds.

In $Li_{999}O_{500}$ and $Li_{1001}O_{500}$, the ionic charge of O was adjusted in order to conserve the charge neutrality of the system. Specifically, the charge of O was set to $-(999 \times [Li\ charge])/500$ in $Li_{999}O_{500}$ and to $-(1001 \times [Li\ charge])/500$ in $Li_{1001}O_{500}$. We confirmed that this small change of the O charge had a negligible influence on the simulation results.

## 3. Results and discussion

### 3.1. Overview of the Li diffusion behavior

The Li diffusion coefficients obtained in $Li_{1000}O_{500}$ (perfect crystal), $Li_{499}O_{500}$ (defective system with 0.1% $Li^+$ vacancies), $Li_{1001}O_{500}$ (defective system with 0.1% $Li^+$ interstitial ions) and $Li_{998}O_{499}$ (defective system with 0.2% $Li^+$ vacancies with 0.2% $O^{2-}$ vacancies as Schottky-type defects) are shown in Fig. 1 (FIT-LDA) and 2 (FIT-EMP), together with the reported experimental values [10]. At low temperatures, the Li diffusivity is clearly enhanced by the defects. It should be noted that the Li diffusivity in $Li_{998}O_{499}$ is lower than that in $Li_{999}O_{500}$, despite the higher concentration of Li defects (0.1% in $Li_{999}O_{500}$ and 0.2% in $Li_{998}O_{499}$). This result derives from the clustering of Li vacancies with an O vacancy in $Li_{998}O_{499}$, although the details will not be discussed in the present paper.

Figs. 1 and 2 also show that Li diffusion coefficients at temperatures near the melting point are comparable with that of the liquid state even before melting. As $Li_2O$ crystal has an anti-fluorite structure, this $PbF_2$-type superionics, which is generally observed in fluorite/anti-fluorite crystals [1], properly emerged under both the FIT-LDA and the FIT-EMP model. The critical temperature was 1500 K under FIT-LDA (Fig. 1) and 1300 K under FIT-EMP

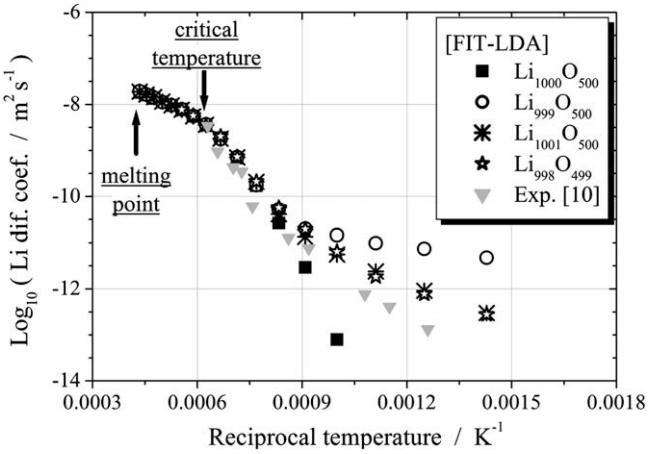


**Fig. 1.** Comparison of the Li diffusion coefficients in $Li_2O$ with/without defects (FIT-LDA), together with the experimental result.

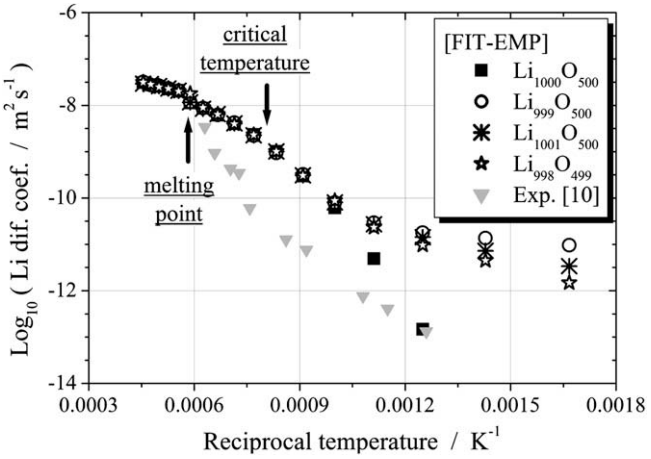


**Fig. 2.** Comparison of the Li diffusion coefficients in $Li_2O$ with/without defects (FIT-EMP), together with the experimental result.

(Fig. 2). The difference in the absolute values resulted from the potential model dependence.

Potential model dependence was also observed in the melting point: 2400 K in FIT-LDA and 1750 K in FIT-EMP. In comparison with the experimental results (1705 K [11]), FIT-LDA overestimated the melting point, while FIT-EMP reproduced it adequately. This tendency is understandable, as FIT-LDA describes inter-ionic interaction more strongly than FIT-EMP [6].

Regarding the relationship between the critical temperature of the superionics ($T_{critical}$) and the melting point ($T_{melt}$), $T_{critical}/T_{melt}$ was 0.63 under FIT-LDA and 0.74 under FIT-EMP. These values are within the general range of the $PbF_2$-type superionics, *i.e.*, 0.6–0.8 [1]. These results indicate a good reliability of both potential models of Li diffusion behavior from the qualitative viewpoint, although significant potential model dependence is seen in some absolute values.

In both models, the diffusion behavior can be divided into four characteristic regions in the defective systems ($Li_{999}O_{500}$, $Li_{1001}O_{500}$ and $Li_{998}O_{499}$): the extrinsic region ($T < 0.8T_{critical}$), the intrinsic region ($0.8T_{critical} < T < T_{critical}$), the superionics region ($T_{critical} < T < T_{melt}$) and the liquid region ($T > T_{melt}$). For the evaluation of the overall Li diffusion coefficient ($D_{Li}$) in the solid state, we considered the former three components:

$$D_{Li} = D_{rd} + D_{td} + D_{df}. \tag{2}$$

Here, $D_{rd}$ corresponds to Li diffusion assisted by radiation defects, $D_{td}$ to that by thermally induced defects excluding dynamic Frenkel defects, and $D_{df}$ to that by dynamic Frenkel defects. Note that, although dynamic Frenkel defects are a type of thermally induced defect, we treated them individually due to their peculiarity.

From the slopes in Figs. 1 and 2, it is reasonable to consider that each component obeys Arrhenius' type formula:

$$D = A \times C \times \exp\left(-\frac{9.65 \times 10^5 E}{RT}\right). \tag{3}$$

Here, $D$ is the diffusion coefficient ($m^{-2}\ s^{-1}$), $A$ the pre-exponential term ($m^2\ s^{-1}$), $C$ the concentration of the defects ([*number of defects*]/[*number of Li atoms*]), $E$ the apparent activation energy for diffusion (eV), $R$ the gas constant (8.31 J $K^{-1}$ $mol^{-1}$), and $T$ is the temperature (K). The parameters $A$, $C$ and $E$ were individually evaluated for $D_{rd}$, $D_{td}$ and $D_{dy}$ as explained in the following sections.

### 3.2. Diffusion assisted by radiation defects ($D_{rd}$)

Li diffusion assisted by radiation defects was further divided into three terms:

**Table 1**
Diffusion parameters (Eq. (3)) for Li diffusion induced by Li vacancies, Li interstitial ions and Schottky-type defects. The asterisked values were evaluated by molecular statics calculation.

| | | $A$ ($m^2\ s^{-1}$) | $E$ (eV) |
|---|---|---|---|
| FIT-LDA | $Li^+$ vac. | $1.74 \times 10^{-7}$ | 0.22, 0.23* [7] |
| | $Li^+$ int. | $4.80 \times 10^{-6}$ | 0.59, 0.56* [7] |
| | Schottky | $2.90 \times 10^{-6}$ | 0.61 |
| FIT-EMP | $Li^+$ vac. | $1.19 \times 10^{-7}$ | 0.13, 0.14* [7] |
| | $Li^+$ int. | $1.15 \times 10^{-6}$ | 0.30, 0.31* [7] |
| | Schottky | $1.23 \times 10^{-6}$ | 0.38 |
| Experiment | Li vac. | – | 0.38 [8] |
| | | | 0.42 [9] |
| DFT calculation | $Li^+$ vac. | – | 0.24* [7] |
| | | | 0.28*–0.33* [10] |
| | $Li^+$ int. | – | 0.53* [7] |

$$D_{rd} = D_{int} + D_{vac} + D_{Sch}. \quad (4)$$

Here, $D_{int}$ corresponds to the diffusion of the Li interstitial ions, $D_{vac}$ to that of the Li vacancies and $D_{Sch}$ to that of the Schottky-type Li defects ($D_{Sch}$). These values were individually evaluated in the $Li_{1001}O_{500}$, $Li_{999}O_{500}$ and $Li_{998}O_{499}$ systems, respectively (Fig. 1). This evaluation was done at 700–1100 K under FIT-LDA and at 600–1000 K under FIT-EMP, because the superionics became dominant at temperatures higher than around half the melting point. The obtained $A$ and $E$ parameters (Eq. (3)) are listed in Table 1.

For both the Li vacancies and the Li interstitial ions, the apparent activation energy for the diffusion was close to the diffusion barrier estimated by molecular statics calculation [6]. In comparison with the experimental results (Li vacancies: 0.38 eV [12], 0.42 eV [13]) and DFT calculation results ($Li^+$ vacancies: 0.24 eV [6], 0.28–0.33 eV [14]; $Li^+$ interstitial ions: 0.53 eV [6]), FIT-LDA gave similar values, while FIT-EMP underestimated the barriers. Correspondingly, FIT-EMP overestimated the Li diffusion coefficients, as shown in Fig. 2.

### 3.3. Diffusion assisted by thermally induced defects ($D_{td}$)

As thermally induced defects, Frenkel defects and Schottky defects are possible. Since it has been reported that the formation energy of Li Frenkel defects is smaller than that of Schottky defects in $Li_2O$ [15], we only considered Frenkel defects for the evaluation of $D_{td}$. Note that these Frenkel defects are not the dynamic Frenkel defects, but the conventional ones. Li Frenkel defects contain the same number of $Li^+$ interstitial ions and $Li^+$ vacancies as Frenkel pairs. Thus, $D_{td}$ can be described as follows:

$$D_{td} = \left\{ A_{int} \times \exp\left(-\frac{E_{int}}{RT}\right) + A_{vac} \times \exp\left(-\frac{E_{vac}}{RT}\right) \right\} \times \left\{ \sqrt{\frac{1}{2}} \times \exp\left(-\frac{E_f}{2RT}\right) \right\}. \quad (5)$$

Here, $E_f$ is the formation energy of the Li Frenkel defects. This value was determined to be 2.33 eV under FIT-LDA and 1.93 eV under FIT-EMP by molecular statics calculation. $A_{int}$, $E_{in}$, $A_{vac}$ and $E_{vac}$ have already been described in Section 3.2.

### 3.4. Diffusion assisted by dynamic Frenkel defects ($D_{df}$)

It is generally considered that the $PbF_2$-type superionics is induced by dynamic Frenkel defects [1]. In the present study, diffusion assisted by dynamic Frenkel defects ($D_{df}$) was estimated in the $Li_{1000}O_{500}$ system at 1200–1500 K under FIT-LDA and at 900–1200 K under FIT-EMP. The diffusion parameters (Eq. (3)) for $D_{df}$ are listed in Table 2. Because the concentration of dynamic Frenkel defects is difficult to define, we kept $C$ at 1 for simplicity. A large pre-exponential part ($A \times C$) is a typical feature of superionics.

**Table 2**
Diffusion parameters (Eq. (3)) for Li diffusion induced by dynamic Frenkel defects.

| | | $A$ ($m^2\ s^{-1}$) | $E$ (eV) |
|---|---|---|---|
| FIT-LDA | Dyn. Frenkel def. | $3.98 \times 10^{-1}$ | 2.42 |
| FIT-EMP | Dyn. Frenkel def. | $2.98 \times 10^{-1}$ | 1.94 |

### 3.5. Modeling of Li diffusion behavior under reactor conditions

In order to model the Li diffusion behavior under fusion-reactor conditions, the overall Li diffusivity ($D_{Li}$) was evaluated by Eq. (1) as a function of the temperature and the concentration of defects. Then, the contribution of different types of diffusion mechanism was estimated as follows:

$$[Contribution\ of\ D_i\ (\%)] = 100 \times \frac{D_i}{D_{Li}} = 100 \times \frac{D_i}{D_{td} + D_{rd} + D_{dy}}, \quad (6)$$

where $D_i$ indicates $D_{td}$, $D_{rd}$ or $D_{dy}$. Here, we assume that (i) radiation defects created by the tritium breeding reaction are Li vacancies or Schottky-type defects, and that (ii) the concentration of these radiation defects is equal to the Li burn-up. These assumptions mean that we ignored the radiation defects induced by collision with fast neutrons as well as high-energy T and He ions. Therefore, the Li diffusivity under low Li burn-up conditions should be underestimated, because the number of radiation defects created by collision would be significant. In addition, we also ignored the annihilation and aggregation of defects. Consequently, the defect concentration should be overestimated at high Li burn-up conditions, because a significant number of Li defects is recovered in reality and the defect concentration would reach a certain saturation level. Although a more sophisticated analysis is required to obtain more reliable quantitative information, the qualitative tendency can be gleaned by the present calculations.

The calculation results for the systems containing 0% Li vacancies (ideal crystal before irradiation), 0.1% Li vacancies (0.1% Li burn-up) and 5% Li vacancies (5% Li burn-up) are shown in Figs. 3 (FIT-LDA) and 4 (FIT-EMP). In the evaluation of the contribution

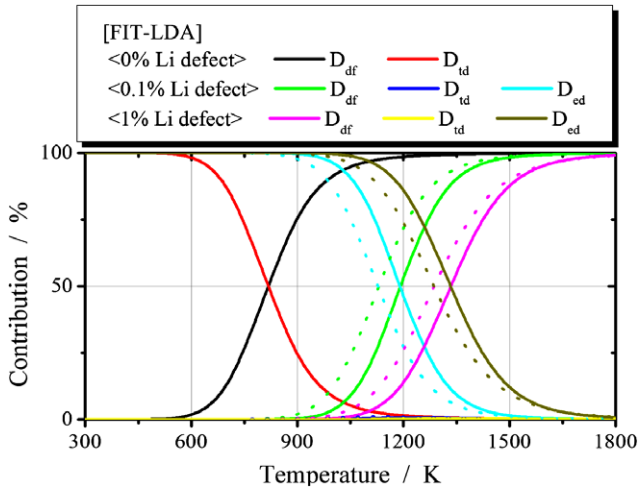


**Fig. 3.** Contribution of $D_{td}$, $D_{df}$ and $D_{rd}$ to the overall Li diffusivity ($D_{Li}$) in the FIT-LDA model. The definition of the contribution is given by Eq. (6). The solid lines represent the results that were obtained in the systems where Li vacancies were introduced as radiation defects, while the dotted lines represent the values that were obtained in the systems where Schottky-type defects were introduced as radiation defects.

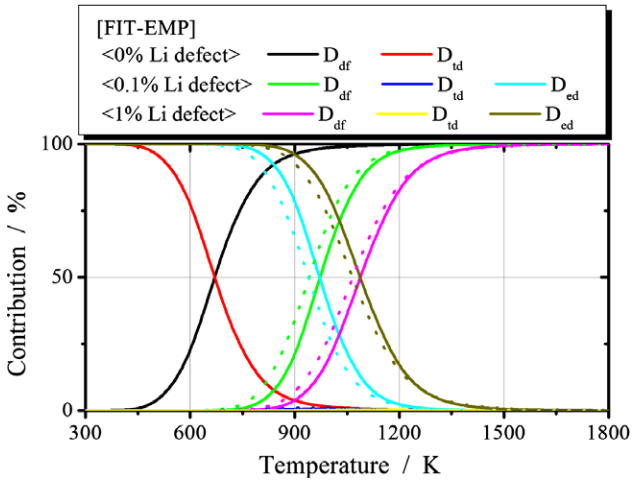


**Fig. 4.** Contribution of $D_{td}$, $D_{df}$ and $D_{rd}$ to the overall Li diffusivity ($D_{Li}$) in the FIT-EMP model. The description format is the same as for Fig. 3.

of $D_{rd}$, the result depends on whether the Li defects created by Li burn-up are Li vacancies or Schottky-type defects. In the present study, both cases were evaluated for comparison. In Figs. 3 and 4, the solid lines represent the results that were obtained in the systems where Li vacancies were introduced, while the dotted lines represent the values that were obtained in the systems where Schottky-type defects were introduced. The following findings were obtained:

- The diffusion assisted by thermally induced defects ($D_{td}$) is negligible except for the ideal crystal.
- Radiation defects govern Li diffusivity at low temperatures (<0.5–0.6 $T_{melt}$), while dynamic Frenkel defects do so at high temperatures (>0.5–0.6 $T_{melt}$).
- Even at low temperatures, dynamic Frenkel defects play a significant role when the Li burn-up is low. As the Li burn-up increases, the contribution of the dynamic Frenkel defects becomes relatively small.
- The temperature at which the diffusion induced by dynamic Frenkel defects becomes dominant is not strongly affected by whether Li radiation defects are Schottky-type defects or Li vacancies.

These results were observed independently of any potential model. Therefore, we consider that they reflect the nature of $Li_2O$, not that of artificial phenomena due to a fault of the potential models.

As for potential model dependence, it was basically observed throughout the present study that the FIT-LDA model tends to overestimate the temperatures for phase transitions, while the FIT-EMP model tends to underestimate them (*e.g.*, the critical temperature of superionics and the melting point). Based on this tendency, we think that the realistic temperature at which the contribution of $D_{df}$ becomes greater than that of $D_{rd}$ is expected to exist between the FIT-LDA and the FIT-EMP results. Even by the inclusion of some variations in the defect concentration so as to compensate for errors due to the assumptions described above, it can be said from Figs. 3 and 4 that both dynamic Frenkel defects and radiation defects play an important roles in Li diffusion in fusion-reactor conditions over a wide Li burn-up range. It is also clear that radiation defects are more influential in systems with higher Li burn-up and lower temperature.

## 4. Conclusion

In order to understand the Li diffusion behavior in lithium-containing oxides under fusion-reactor conditions, a classical molecular dynamics simulation was conducted for $Li_2O$. Dynamic Frenkel defects, which are thought to cause superionics, mainly assisted Li diffusion at temperatures higher than about half the melting point. In systems containing Li defects such as Li vacancies and Schottky-type defects, Li diffusion was promoted by these defects. It was indicated that both dynamic Frenkel defects and radiation defects have significant contributions to Li diffusion in fusion-reactor conditions. It was also indicated that radiation defects play a more important role in systems with higher Li burn-up and lower temperature.

## References

[1] S. Hull, Rep. Prog. Phys. 67 (2004) 1233.
[2] T.W.D. Farley, W. Hayes, S. Hull, M.T. Hutchings, M. Vrtis, J. Phys. Condens. Matter 3 (1991) 4761.
[3] S. Hull, T.W.D. Farley, W. Hayes, M.T. Hutchings, J. Nucl. Mater. 160 (1988) 125.
[4] J. Habasaki, Y. Hiwatari, Phys. Rev. B 69 (2004) 144207.
[5] J.G. Rodeja, M. Meyer, M. Hayoun, Model. Simul. Mater. Sci. Eng. 9 (2001) 81.
[6] T. Oda, Y. Oya, S. Tanaka, W.J. Weber, J. Nucl. Mater. 367–370 (2007) 263.
[7] W. Smith, T. Forester, J. Mol. Graph. 14 (1996) 136.
[8] M.P. Allen, D.J. Tildesley, Computer Simulation of Liquids, Clarendon, Oxford, 1989.
[9] H.J.C. Berendsen, J.P.M. Postma, W. van Gunsteren, A. DiNola, J.R. Haak, J. Chem. Phys. 81 (1984) 3684.
[10] Y. Oishi, Y. Kamei, M. Akiyama, J. Nucl. Mater. 87 (1979) 341.
[11] Y.Y. Liu, M.C. Billone, A.K. Fischer, S.W. Tam, R.G. Clemmer, G.W. Hollenberg, Fusion Technol. 8 (1985) 1970.
[12] T. Matsuo, H. Ohno, K. Noda, S. Konishi, H. Yoshida, H. Watanabe, J. Chemical Society, Faraday Trans. II 79 (1983) 1205.
[13] H. Ohno, S. Konishi, K. Noda, H. Takeshita, H. Yoshida, H. Watanabe, J. Nucl. Mater. 118 (1983) 242.
[14] M. Wilson, S. Jahn, P.M. Madden, J. Phys. Condens. Mater. 16 (2004) S2795.
[15] K. Ando, M. Akiyama, Y. Oishi, J. Nucl. Mater. 95 (1980) 259.